Analysis of the steady-state axial flow in the Hall thruster

Avi Cohen-Zur
Faculty of Aerospace Engineering, Technion-Israel Institute of Technology, Haifa 32000, Israel and Holon Academic Institute of Technology, P.O. Box 305, Holon 58102, Israel

Amnon Fruchtman[a)]
Holon Academic Institute of Technology, P.O. Box 305, Holon 58102, Israel

Joseph Ashkenazy
Propulsion Physics Laboratory, Soreq NRC, Yavne 81800, Israel

Alon Gany
Faculty of Aerospace Engineering, Technion-Israel Institute of Technology, Haifa 32000, Israel

(Received 10 June 2002; accepted 31 July 2002)

Momentum and energy balance considerations are used to analyze the plasma flow in a Hall thruster at the limit of intense full ionization with no losses. Two cases are examined; one in which the ion velocity at the anode is zero, and the second in which an ion backflow exists near the anode. Analytical expressions are found for the current utilization and for the thruster efficiency in each case. In the first case an expression is also found for the electron temperature at the anode, while in the second case expressions are derived for the magnitude of the ion backflow into the anode and for the location of the ionization region along the channel. These dependencies are expressed in terms of the applied magnetic field and voltage, the mass flow rate, the thruster geometry and the ionization energy. © *2002 American Institute of Physics.* [DOI: 10.1063/1.1508774]

I. INTRODUCTION

Hall thrusters, a type of electric thrusters that are used for propulsion of space vehicles,[1–3] perform with efficiencies of more than 50% in the important range of specific impulses of 1500–2500 seconds. There is a substantial interest in improving the Hall thruster performance in terms of a better plume collimation, operation extending to both higher and lower regimes of power and thrust, and variable thrust. Understanding the structure of the plasma flow in the thruster could be useful for accomplishing this task. Our efforts towards achieving such an understanding have resulted, in recent years, in the development of a one-dimensional steady-state model of the Hall thruster and in the demonstration that a smooth acceleration of the flow to supersonic velocities is possible inside the thruster channel.[4–7] This work also led to the suggestion of ways to deliberately generate an abrupt sonic transition inside the channel.[7] Additional aspects of the sonic transition have been addressed by other scientists.[8–10]

In a recent one-dimensional analysis of the Hall thruster at the limit of intense full ionization with no losses Ahedo, Martinez-Cerezo, and Martinez-Sanchez[11] have identified the different processes that are dominant in distinct different regions along the thruster. They performed a numerical calculation for a set of parameter values that corresponds to an SPT-100 class thruster[12] followed by an asymptotic analysis in which relations between various flow parameters were derived. This ideal case results from the assumption of no losses and is characterized by a high electron temperature. In the case of a high enough mass flow rate, the high electron temperature causes the ionization to occur only in a narrow layer that is separated from the regions of ion acceleration. In a more recent analysis[13] Ahedo *et al.* included losses at lateral walls and heat conduction and showed that accounting for these additional processes makes the division of the flow into distinct regions less apparent and the electron temperature lower. Other theoretical calculations that include wall losses, such as those performed by Makowski *et al.*,[9] by Choueiri,[14] and by Keidar *et al.*,[15] also showed lower electron temperatures. Despite the not-so-realistic nature of the assumption of no losses the study of this ideal case provides an insight into the governing processes in the thruster.

Our purpose in this paper is to pursue the investigation of the Hall thruster at the limit of intense full ionization with no losses in order to gain further insight into the physical processes that govern the flow. Employing momentum and energy balance considerations, we derive analytical expressions for the dependence of the flow variables and the thruster efficiency on the profile and intensity of the applied magnetic field, on the applied voltage, on the mass flow rate, on the thruster geometry and on the ionization energy of the propellant.

The calculated flow crucially depends on the ion velocity specified at the anode. In certain studies the ion velocity was assumed to be supersonic immediately upon entering the channel.[15,16] Since the ionization occurs mostly where the flow is still subsonic, in our investigation we have usually chosen the boundary condition that the ion velocity is zero upon entering the channel (at the anode).[4,5,7,9] In contrast, Ahedo *et al.*, in their analysis mentioned above,[11,13] have assumed that an electron-repelling sheath exists near the anode and have imposed the requirement that the Bohm condition[17]

[a)]Electronic mail: fnfrucht@hait.ac.il

be satisfied at the sheath edge. As a result of these assumptions, they have found, for the first time theoretically, steady-state flows that include a backflow towards the anode, similar to the backflow claimed in the past.[18,19] Recently, Dorf *et al.* have suggested that the existence of a sheath near the anode and the value of the ion velocity there depend on the applied voltage and the plasma parameters.[20] It is still not clear what the actual ion velocity at the anode is. Without resolving this important issue, we examine in our analysis here both possible cases: zero ion velocity at the anode and ion backflow towards the anode. In both cases the assumptions of intense full ionization and absence of losses result in the formation of a narrow ionization layer. If the ion velocity at the anode is zero the ionization layer is attached to the anode, while if ion backflow towards the anode exists the ionization layer is detached from the anode and separates the acceleration region from the backflow region.

At the limit of intense ionization with no losses the efficiency is only reduced due to a less-than-unity current utilization. In this ideal case the propellant utilization, the fraction of gas that ends up being ionized upon exiting the thruster, turns out to be unity. Moreover, the electric potential in the ionization layer is close to the anode potential, resulting in the energy utilization being nearly unity as well. The channel cross section is assumed constant at all axial positions, resulting in no efficiency reduction due to a plume diversion. One of our goals is thus to derive an analytical expression for the current utilization, and therefore, for the total efficiency.

A full current utilization that corresponds to a hundred percent efficiency, fulfilled when all the dissipated electric power is used for ion acceleration only, is impossible. A certain amount of power has to be dissipated in the electron current. It heats up the electrons and, consequently, is used for production, through ionization, of the ions that generate thrust. This necessary power sink sets a limit on the current utilization and on the efficiency. An excess of power above that amount, however, results in a further, undesired reduction of the current utilization and of the efficiency. In the case of a zero ion velocity at the anode this reduction is expressed in a finite temperature of the electrons that reach the anode. In the second case, the reduction is expressed through the production of an ion backflow towards the anode. These ions do not contribute to the thrust, rather they recombine upon reaching the anode after flowing back from the ionization layer. We derive analytical expressions for the electron temperature at the anode and for the backflow current.

In Sec. II we present the model. In Sec. III we present two flows calculated numerically for the same set of control parameters, but for the two different boundary conditions at the anode discussed above. In Sec. IV we derive analytical relations for the two flows, which we compare with numerical calculations in Sec. V. The results are discussed in Sec. VI.

II. THE MODEL

In this section we describe the one-dimensional model employed for analyzing the flow in the Hall thruster at the limit of intense full ionization with no losses. Inspired by the recent results of Ahedo *et al.*,[11] we adopt some of their notations and, in the next section, address a problem with similar values of the control parameters.

The ion dynamics is governed by the continuity equation

$$\frac{d}{dz}(nv_i)=\frac{d}{dz}(nv_e)=-\frac{d}{dz}(n_a v_a)=\beta n n_a, \tag{1}$$

and by the momentum equation

$$\frac{d}{dz}(m_i n v_i^2)=-en\frac{d\phi}{dz}, \tag{2}$$

where n and n_a are the densities of the quasi-neutral plasma and neutral gas; v_i, v_e, and v_a are the ion, electron, and neutral average velocities in the z direction; e and m_i are the ion charge and mass, and ϕ is the electrostatic potential. We assume that the main variation in the coaxial geometry of the thruster is along z, the axial coordinate. The ions are assumed cold, collisionless and unmagnetized. The plasma is generated by ionizing collisions between electrons and neutral atoms at a rate per unit volume $\beta n n_a$, where $\beta \equiv \langle \sigma v \rangle$, σ being the ionization cross section and the notation $\langle\ \rangle$ represents averaging over the distribution function of v, the electron velocity. In writing Eq. (1) we assumed that the cross section of the thruster is uniform along the channel, while in writing Eq. (2) we neglected the small momentum of the neutrals. We make these two assumptions throughout the paper. The axial component of the electron momentum equation is

$$0=en\frac{d\phi}{dz}-\frac{d(nT)}{dz}-j_\theta B, \tag{3}$$

where T is the electron temperature, j_θ is the electron azimuthal current density, B is the intensity of the approximately radial applied magnetic field, and the electron inertia is neglected. Adding Eqs. (2) and (3), we obtain the momentum balance equation

$$\frac{d}{dz}(m_i n v_i^2+nT)=-j_\theta B. \tag{4}$$

The particle total pressure (the term in brackets on the left hand side of the equation) is changed by the external force, which is the magnetic field force only. In the quasi-neutral plasma the net electric field force is negligible relative to the net magnetic field force. From the θ component of the electron momentum equation we obtain $j_\theta B=-m_e \nu_d j_e/e$ ($\nu_d \equiv \omega_c^2/\nu$). Here m_e, ω_c, ν and $j_e \equiv -env_e$ are the electron mass, cyclotron frequency, collision frequency and axial current density. It is assumed that $\nu \ll \omega_c$. Employing this last relation we obtain the momentum balance equation in a more useful form

$$\frac{d}{dz}(m_i n v_i^2+nT)=\frac{m_e \nu_d j_e}{e}. \tag{5}$$

Integrating Eq. (5) along the thruster we obtain

$$(m_i n v_i^2)_C = (m_i n v_i^2)_A + (nT)_A - (nT)_C + \int_A^C \frac{m_e \nu_d j_e}{e} dz. \tag{6}$$

The net thrust [the left hand side of Eq. (6)] is the sum of thrust due to the ion backflow that impinges on the anode, the difference between the particle pressure at the two ends of the thruster and the magnetic field force exerted on the plasma. Here the subscripts A and C denote the values of the quantities at the locations of the anode and the cathode, respectively.

From Eq. (1) it follows that the sum of the ion and atom fluxes is uniform along the channel. This sum is

$$(n v_i + n_a v_a) S = \frac{\dot{m}}{m_i}, \tag{7}$$

where $\dot{m}$ is the mass flow rate and S is the channel cross section. In this paper we assume that v_a is uniform in the channel, and therefore, Eq. (7) determines the value of the varying neutral density n_a along the channel as a function of the varying ion flux density $n v_i$.

The equation that governs the evolution of the electron enthalpy is

$$n v_e \frac{d}{dz}\left(\frac{5}{2}T\right) = e n v_e \frac{d\phi}{dz} - \beta n n_a \left(\alpha_i \epsilon_i + \frac{5}{2}T\right), \tag{8}$$

where ϵ_i is the ionization energy and $\alpha_i \epsilon_i$ is the average energy cost for ionization. Generally α_i is a function of the electron temperature and decreases when T increases, expressing the fact that a larger fraction of the electron inelastic collisions end up in ionizations and a smaller fraction in excitations.[21] Wall losses, recombination and heat conduction are neglected in the ideal case we assume here. Multiplying Eq. (2) by v_i and adding the resulting equation to Eq. (8), we obtain an equation for the total energy balance:

$$\frac{d}{dz}\left(\frac{m_i n v_i^3}{2} + \frac{5}{2} n v_e T + n v_i \alpha_i \epsilon_i + j_D \phi\right) = -\beta n n_a \frac{m_i v_i^2}{2}, \tag{9}$$

where $j_D = en(v_i - v_e)$ is the discharge current density.

We do not calculate the evolution of the flow beyond the cathode, nor do we allow a varying cross section of the plasma flow. Rather, we restrict ourselves to the analysis of the assumed constant-cross-section flow between the anode located at $z=0$ and the cathode (that coincides with the exit plane) at $z=L$. The boundary conditions that we specify are the electron temperature at the exit plane (which is the temperature of the electrons emerging from the cathode T_C), the potential drop between the anode and the cathode (the applied voltage ϕ_A), and the ion velocity at the anode v_A

$$T(z=L) = T_C; \quad \phi(z=0) = \phi_A, \quad \phi(z=L) = 0;$$
$$v_i(z=0) = v_A. \tag{10}$$

We also require that there be a smooth acceleration to supersonic velocities towards the exit. The result of imposing these requirements is that the electron current emitted from the cathode (or the discharge current) is determined as an eigenvalue.[4,5,7]

As mentioned above, we are interested in two cases. For the first case we assume that the ion velocity at the anode is zero

$$v_A = 0. \tag{11a}$$

For the second case, we adopt the assumption that an electron-repelling sheath exists near the anode. We solve the quasi-neutral equations up to the edge of the sheath. the sheath is assumed to be narrow, so that the ion velocity at the anode is taken as the Bohm (ion acoustic) velocity towards the anode

$$v_A = -c_s \equiv -\sqrt{\frac{5T}{3m_i}}, \tag{11b}$$

and the potential at the anode is taken as the sheath potential $\phi_{\rm sh}$ above ϕ_A

$$\phi(z=0) = \phi_A + \phi_{\rm sh}, \tag{12}$$

where

$$\phi_{\rm sh} = \frac{T_A}{e} \ln\left(\sqrt{\frac{3m_i}{10\pi m_e}} \frac{j_{bf}}{j_{eA}}\right). \tag{13}$$

Here $T_A = T(z=0)$ is the temperature at the anode that is not specified but rather solved for, j_{bf} is the ion current density at the anode (the backflow current density), and j_{eA} is the electron current density at the anode.

Once the flow parameters are calculated the efficiency can be determined. The total efficiency η_D is the product of the propellant utilization η_m, the energy utilization η_E, and the current utilization η_C

$$\eta_D = \eta_m \eta_E \eta_C, \tag{14}$$

where the various utilizations are defined as

$$\eta_m \equiv \frac{m_i S j_i(z=L)}{e\dot{m}}, \quad \eta_E = \left[\frac{v_i(z=L)}{v_0}\right]^2,$$
$$\eta_C = \frac{j_i(z=L)}{j_D}. \tag{15}$$

Here $j_i = en v_i$ is the ion current density and $v_0 \equiv \sqrt{2e\phi_A/m_i}$.

III. TWO NUMERICAL EXAMPLES

In this section we calculate the flow for which the values of the control parameters correspond to an SPT-100 class thruster.[12] The axial profile of the magnetic field, the dependence of β on the electron temperature, the electron collisionality and α_i have the same forms as in Ref. 11. For simplicity we assume a flow of a constant cross section in which no plume develops. The calculation demonstrates the features of the plasma flow at the limit of intense ionization, features that are exhibited in the next section by the analytical results.

The distance between the anode and the cathode is $L = 50$ mm and the assumed constant cross section of the channel is $S = 45$ cm^2. The magnetic field is assumed to point in the radial direction and to have a dependence on the axial coordinate in the form

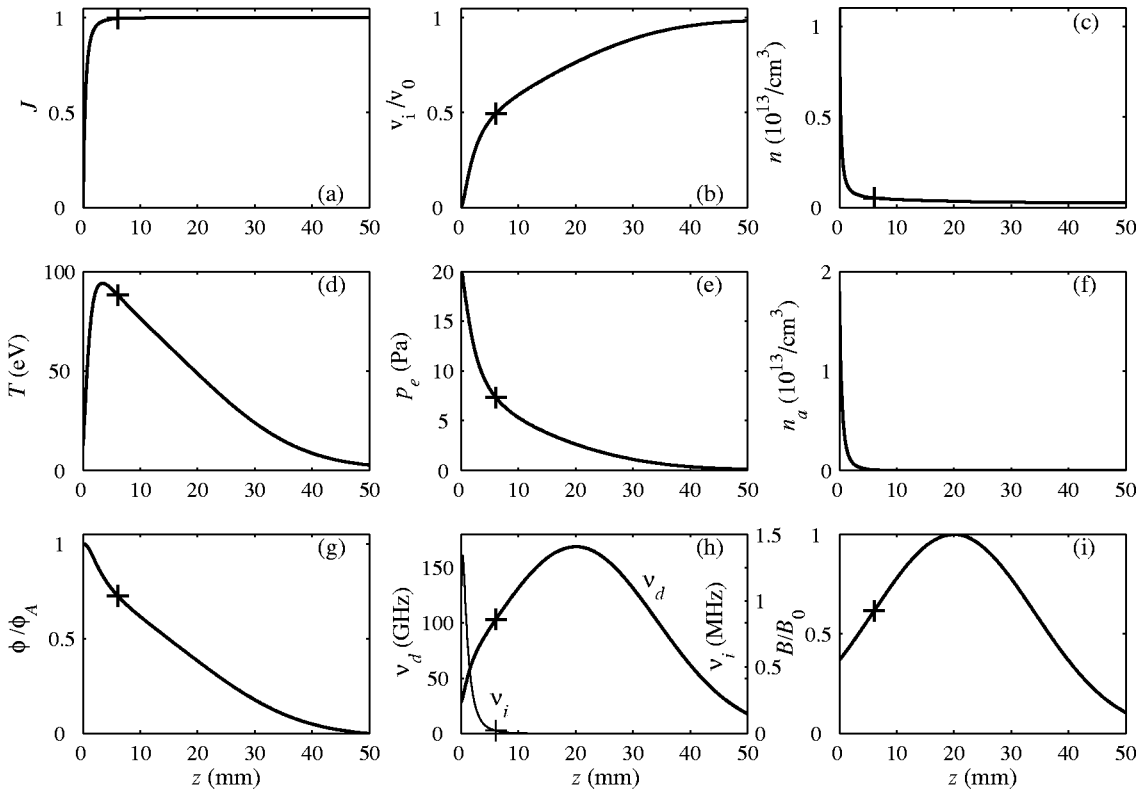

FIG. 1. Calculated profiles of flow variables in the Hall thruster (zero ion velocity at the anode): $S=45$ cm^2, $L=50$ mm, $z_m=20$ mm, $L_m=20$ mm, $\dot{m}=5.32$ mg/s, $\phi_A=300$ V, $B_0=120$ G, $\alpha_i=2.5$. Denoted is z_s, the location of the sonic transition.

$$B=B_0\exp\left[-\frac{(z-z_m)^2}{L_m^2}\right], \tag{16}$$

with $z_m=20$ mm and $L_m=20$ mm. This form of the supposedly curl–free magnetic field is only approximate. The magnetic field intensity as a function of z is shown in Figs. 1(i) and 2(i).

The propellant is Xenon with ionization energy $\epsilon_i=12.1$ eV, and α_i is taken as a constant, $\alpha_i=2.5$. The dependence of β on the electron temperature is approximated by

$$\beta=v_{te}\sigma_{i0}\left[1+\frac{\epsilon_i/T}{(1+\epsilon_i/T)^2}\right]\exp(-\epsilon_i/T), \tag{17}$$

where $\sigma_{i0}=5\times10^{-20}$ m^2 and $v_{te}=\sqrt{8T/(\pi m_e)}$ is the electron thermal velocity. We write the electron collisionality as

$$\nu=\nu_{en}+\nu_{ano}, \tag{18}$$

where ν_{en} is the electron–neutral collision frequency, ν_{ano} is the anomalous collision frequency, and electron–ion collisions are neglected. The collision frequencies are

$$\nu_{en}=n_a\sigma_{en}v_{te}, \quad \nu_{ano}=\alpha_B\omega_c, \tag{19}$$

where σ_{en} is approximated as $\sigma_{en}=27\times10^{-20}$ m^2, and Bohm diffusion is the anomalous diffusion mechanism, the Bohm parameter is chosen to be $\alpha_B=1/80$.

Equations (1), (2), (5), (7), and (8) are singular at the sonic velocity, but admit regular solutions in which there is a smooth acceleration to supersonic velocities towards the cathode. We find such regular solutions that satisfy the boundary conditions (10) by numerically integrating the equations from the sonic transition plane towards both anode and cathode, as described in Refs. 4, 5, and 7. The values of the control parameters in the numerical examples are $\dot{m}=5.32$ mg s^{-1}, $\phi_A=300$ V, $B_0=120$ G, and $T_C=2.7$ eV.

In Figs. 1 and 2 we present the calculated profiles of the flow variables for the two sets of boundary conditions. Figure 1 shows the profiles of the flow parameters in the case of zero velocity at the anode. These profiles are similar to the profiles found in our previous investigations.[4,5,7] The channel is divided into a narrow ionization layer attached to the anode and a long acceleration region. The sonic plane is placed near the downstream edge of the ionization layer where the ionization rate is just sufficiently high to meet the regularity condition for a smooth sonic transition. The sonic transition plane at the boundary between the two regions is denoted in the figure. The narrow, intense ionization layer causes the ion current to increase to nearly the maximal possible value (at full ionization), and results in an acceleration region in which the plasma is almost completely ionized and accelerates to almost the maximal velocity available by the applied voltage. There are almost no neutrals present in the acceleration region.

Figure 2 shows the profiles of the flow parameters in the case of a backflow towards the anode. The division into three distinct regions is apparent in Fig. 2. As pointed out by Ahedo *et al.*,[11] in addition to the ionization and acceleration regions there is a third region, a long diffusion region adjacent to the anode that includes an anode presheath, with a

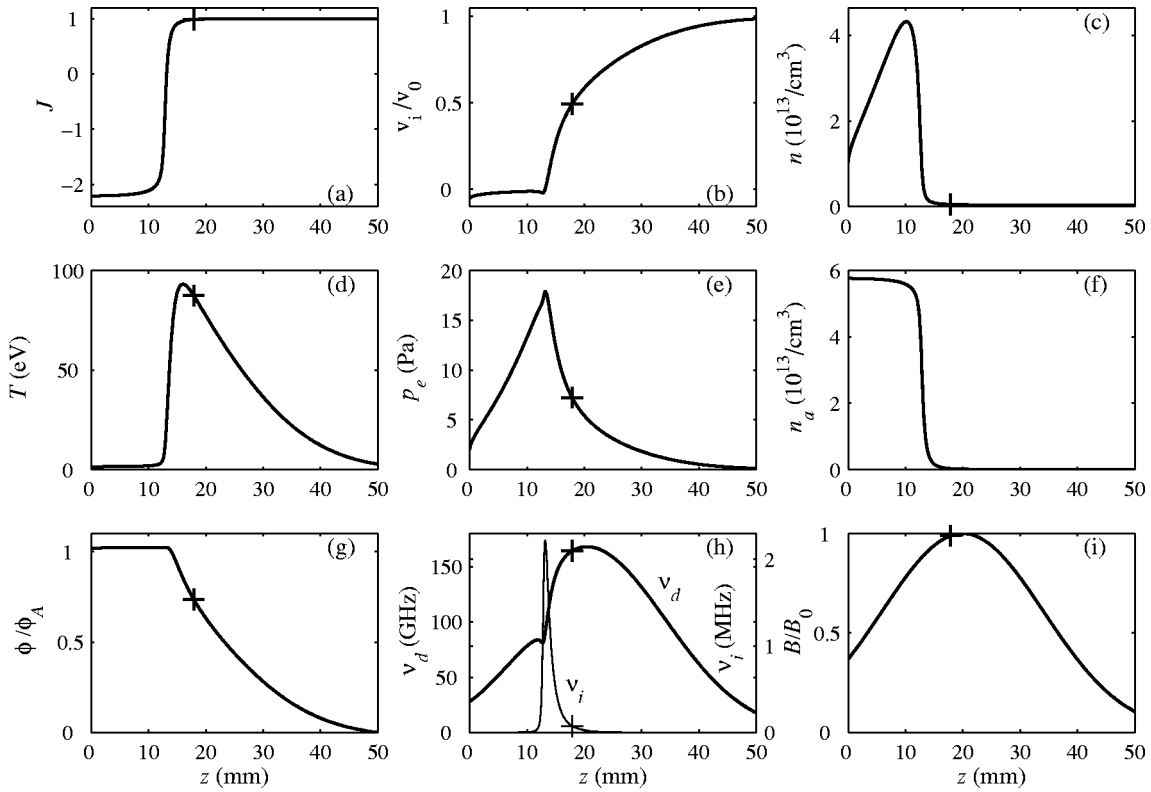

FIG. 2. Calculated profiles of flow variables in the Hall thruster (ion backflow case). The values of the parameters are as those in Fig. 1. Denoted is z_s, the location of the sonic transition.

slow ion backflow, a low electron temperature and a weak electric field. In contrast to the case shown in Fig. 1, the electric potential in Fig. 2 is nonmonotonic and the ion velocity in the diffusion region is negative; the ions flow towards the anode. In this second case the narrow, intense ionization causes all the gas to be ionized and to experience a maximal acceleration in the acceleration region, as it does in the first case, but also causes a sharp drop of the electron temperature anodewise. The intense ionization results, therefore, in the ionization layer being bounded by a low temperature region at the anode side and a region with no neutrals at the cathode side.

In both cases shown in Figs. 1 and 2 the intense ionization and the assumption of no losses result in all the gas being ionized, so that

$$nv_i \simeq \frac{\dot{m}}{Sm_i}, \tag{20}$$

or $J \equiv m_i S j_i/(e\dot{m}) \simeq 1$ at the edge of the narrow ionization layer, and

$$\eta_m \simeq 1. \tag{21}$$

Also, the ions are being accelerated by the full applied voltage, so that

$$v_i(z=L) \simeq v_0 \tag{22}$$

and

$$\eta_E \simeq 1. \tag{23}$$

The total efficiency becomes, therefore, the current utilization that turns out to be

$$\eta_D \simeq \eta_C \simeq 1/J_D, \tag{24}$$

where $J_D \equiv m_i S j_D/(e\dot{m})$. Numerically, in the first case the normalized discharge current density and the total efficiency are found to be $J_D = 1.2051$ and $\eta_D = 0.8035 \cong 1/J_D = 0.8298$. In the second case the normalized discharge current density and the total efficiency are $J_D \cong 1.3272$ and $\eta_D = 0.7303 \cong 1/J_D = 0.7534$. In none of these two cases does the efficiency attain its maximal value. In the first case T_A is nonzero ($T_A = 12.82$ eV), while in the second case j_{bf} is nonzero ($j_{bf} = -2.208\ e\dot{m}/Sm_i = 0.1905$ A/cm^2).

The distinct regions in which different processes are dominant allow the derivation of simple relations between various flow quantities. In the next section we use the momentum and energy balance equations to derive these simple relations which give rise to analytical expressions that enable us to predict the main features of the flow and the thruster performance, as a function of the control parameters.

IV. ANALYTICAL EXPRESSIONS

As we have seen in the numerical examples presented in Figs. 1 and 2, at the limit of intense full ionization with no wall losses the channel is composed of a narrow ionization layer and an acceleration region, while when there exists an ion backflow, the backflow region is located between the anode and the narrow ionization layer. The electron and ion current densities are constant except across the narrow ion-

ization layer. In the acceleration region the electron current density equals the density of the electron current emitted from the cathode j_{eC}, and, following Eq. (20), we approximate the ion flux in the acceleration region as the atom flux injected at the anode. Following Eq. (22) we assume that the ions are accelerated by the full applied voltage. We, therefore, write for the acceleration region

$$j_e = j_{eC}, \quad n v_i = \frac{\dot{m}}{S m_i}, \quad v_i(z=L) = v_0. \tag{25}$$

We first derive approximate relations from the momentum balance relations [Eq. (5)]. These approximate relations are similar to those derived in Ref. 11, but allow a nonuniform ν_d. Later, additional approximate relations will be derived from the energy balance equations.

By integrating Eq. (5) across the acceleration region, we obtain

$$\frac{\dot{m}}{S} v_0 - (nT)_{\text{peak}} = \frac{m_e}{e} j_{eC} \int_{z_{\text{peak}}}^{L} dz \nu_d, \tag{26}$$

where z_{peak} denotes the location of the potential peak and $(nT)_{\text{peak}}$ is the electron pressure at $z = z_{\text{peak}}$. The potential peak is located inside the ionization layer. Since the ionization layer is narrow, it is a good approximation to assume that $j_e = j_{eC}$ throughout the region of integration and not only in the acceleration region. The electron pressure at the cathode $(nT)_C$ is neglected since

$$(nT)_C \ll \frac{\dot{m}}{S} v_0. \tag{27}$$

The ion velocity at the potential peak inside the ionization layer is assumed zero (since, as mentioned above, we neglect the small velocity of the gas atoms). Therefore, Eq. (26) relates the plasma momentum at the channel exit to the change along the channel of the total pressure (the sum of the particle pressure and the magnetic field pressure). In the case in which the ion velocity at the anode is zero, $z_{\text{peak}} = 0$, while in the case of a backflow z_{peak} is somewhere between the electrodes.

For the derivation of the second relation we use the following: In the acceleration region the ion and electron fluxes are constant. Equations (2) and (8) then yield $m_i v_i^2/2 + 5T/2 = e\phi_A$. At the sonic transition, that occurs at the edge of the ionization region,[4–10] $m_i v_s^2/2 = 5T_s/6$ (quantities at the sonic transition plane are denoted by the subscript s). Substituting this expression into the above equation yields $T_s = 3e\phi_A/10$ and $v_s = \sqrt{e\phi_A/(2m_i)} = v_0/2$. These relations were also derived in Ref. 11. Since a smooth sonic transition requires that ionization there is not zero, the sonic transition has to occur close to the ionization layer, and $n_s(m_i v_i^2 + T)_s = (nT)_{\text{peak}}$. Substituting $n_s = \dot{m}/(S m_i v_s) = 2\dot{m}/(S m_i v_0)$ and $(m_i v_i^2 + T)_s = (4/5) e\phi_A$ into this last equation yields the sought-after second relation

$$(nT)_{\text{peak}} = \frac{4}{5} \frac{\dot{m}}{S} v_0. \tag{28}$$

Combining Eqs. (26) and (28) we obtain the relation

$$\frac{1}{5} \frac{\dot{m}}{S} v_0 = \frac{m_e}{e} j_{eC} \int_{z_{\text{peak}}}^{L} dz \nu_d. \tag{29}$$

In the case that the ion velocity at the anode is zero this relation determines j_{eC}, and therefore, the cathode current, the discharge current and the efficiency (assuming ν_d is known). The electron temperature at the anode is still not determined by the momentum balance.

We turn now to analyze the region between the anode and the peak of the potential. Whenever the peak of the potential is not located at the anode there is a backflow. In the region of the backflow, the flow is subsonic except at the anode itself. It is, therefore, a good approximation to neglect the ion momentum and to write the integrated form of Eq. (5) as a balance between the magnetic field pressure and the particle pressure

$$(nT)_{\text{peak}} - (nT)_A = \frac{m_e}{e} j_{eA} \int_0^{z_{\text{peak}}} dz \nu_d, \tag{30}$$

or, employing Eq. (28), as

$$\frac{4}{5} \frac{\dot{m}}{S} v_0 - (nT)_A = \frac{m_e}{e} j_{eA} \int_0^{z_{\text{peak}}} dz \nu_d. \tag{31}$$

In writing this form we assume that the region of ionization of the backflow is a small part only of the whole backflow region. Therefore, we assumed that the electron current density along most of this region is j_{eA}, the electron current density at the anode. We can express the electron currents by the discharge current density j_D, the backflow ion current density j_{bf} and the gas mass flow rate per unit area $\dot{m}/S$, as

$$j_{eC} = j_D - \frac{e\dot{m}}{S m_i}, \quad j_{eA} = j_D - j_{bf}, \tag{32}$$

where Eq. (20) was used. The backflow current j_{bf} is zero in the case of zero ion velocity at the anode and negative in the case of a backflow. In the absence of a backflow, the peak of the potential is located at the anode, $(nT)_A = (4/5)\dot{m} v_0/S$, and Eq. (31) is trivially satisfied.

Adding Eqs. (26) and (30) we obtain an approximated form of Eq. (6)

$$\frac{\dot{m}}{S} v_0 = (nT)_A + \frac{m_e}{e} j_{eA} \int_0^{z_{\text{peak}}} dz \nu_d + \frac{m_e}{e} j_{eC} \int_{z_{\text{peak}}}^{L} dz \nu_d. \tag{33}$$

The thrust [the left hand side of Eq. (33) multiplied by S] is the maximal possible thrust and is determined by the mass flow rate, the ion mass, and the applied voltage. This thrust is the sum of contributions from the plasma pressure at the anode and the magnetic field force.

Examining Eqs. (29), (31), and (32) we notice that even if ν_d is known there are still four unknowns in these two equations: z_{peak}, j_D, j_{bf}, and $(nT)_A$. In addition to the momentum balance, energy balance has to be used in order to enable us to determine the values of these unknowns. Energy balance is also necessary in order to estimate the electron temperature at the anode in the case of a zero ion velocity. In the following we turn to an analysis of the energy balance.

We assume that the ion ''heating'' due to ionization [the right hand side of Eq. (9)] is small. Integrating Eq. (9) along the channel yields

$$\Gamma_E \equiv \frac{m_i n v_i^3}{2} + \frac{5}{2} n v_e T + n v_i \alpha_i \epsilon_i + j_D \phi = \text{const}. \tag{34}$$

Let us write the expressions for the Γ_E at several locations: At the cathode, at the anode, and at the peak of the potential. For writing Γ_E at the cathode we employ in the first term of the expression (34), Eqs. (25) and (23), and neglect the second term since T at the cathode is much smaller than $\alpha_i \epsilon_i$. The energy flux density at the cathode, where $\phi = 0$, turns out to be $\Gamma_{E,C} = \dot{m}/(S m_i)(e\phi_A + \alpha_i \epsilon_i)$.

At the anode the potential is $\phi = \phi_A$ while the ion velocity is either zero (in the absence of a backflow) or finite but small (in the presence of a backflow). In both cases we neglect the first term in the expression (34) since $m_i v_i^2/2$ at the anode is much smaller than $\alpha_i \epsilon_i$. Employing (32) we express the energy flux density at the anode as $\Gamma_{E,A} = (5/2)(j_{bf} - j_D) T_A/e + j_{bf} \alpha_i \epsilon_i / e + j_D \phi_A$. We write the equality $\Gamma_{E,C} = \Gamma_{E,A}$ in the form

$$-\frac{5}{2}\frac{(j_{bf} - j_D)}{e} T_A - \frac{j_{bf}}{e} \alpha_i \epsilon_i + \frac{\dot{m}}{S m_i}(e\phi_A + \alpha_i \epsilon_i) = j_D \phi_A . \tag{35}$$

The equation in this last form states that in the ideal case with no losses the power applied to the thruster is used for ionization [$(\dot{m}/S m_i)\alpha_i \epsilon_i$ for the gas that is accelerated towards the exit, and $-j_{bf} \alpha_i \epsilon_i / e$ for the gas that flows backwards towards the anode], $(\dot{m}/S m_i) e \phi_A$ for acceleration towards the exit, and $-(5/2)(j_{bf} - j_D) T_A/e$ for heating the electrons to the temperature at which they reach the anode.

We can also estimate the plasma density and the electron temperature at the peak of the potential. The peak of the potential is either located at the anode, in the absence of backflow, or inside the ionization layer having a value slightly above ϕ_A, in the presence of a backflow. We approximate for both cases $\phi_{\text{peak}} = \phi_A$. The ion velocity and the ion flux are zero at the location of the potential peak, so that the discharge current there is carried by the electrons only, $(n v_e)_{\text{peak}} = -j_D/e$. We denote the electron temperature there as $T = T_{\text{peak}}$, which, in the case of no backflow, is equal to T_A, the anode temperature. Substituting these values into Eq. (34), we obtain $\Gamma_{E,\text{peak}} = -(5/2)(j_D/e) T_{\text{peak}} + j_D \phi_A$. We can write $\Gamma_{E,C} = \Gamma_{E,\text{peak}}$ in the form

$$-\frac{5}{2}\frac{j_D}{e} T_{\text{peak}} + j_D \phi_A = \frac{\dot{m}}{S m_i}(e\phi_A + \alpha_i \epsilon_i). \tag{36}$$

This equation determines T_{peak}, once j_D is found. Using Eq. (28) we express the plasma density at the potential peak n_{peak} as

$$n_{\text{peak}} = \frac{(nT)_{\text{peak}}}{T_{\text{peak}}} = \frac{4}{5}\frac{\dot{m}}{S}\frac{v_0}{T_{\text{peak}}}. \tag{37}$$

We note that in the case of no backflow Eq. (35) is reduced to Eq. (36), so that $T_{\text{peak}} = T_A$, and n_{peak} is the plasma density at the anode.

For convenience we write the governing equations, Eqs. (29), (31), (35)–(37), in the following dimensionless form:

$$\tfrac{1}{5} = (J_D - 1) F (1 - f), \tag{38}$$

$$\tfrac{4}{5} - P_A = (J_D - J_{bf}) F f, \tag{39}$$

$$\tfrac{5}{2}(J_D - J_{bf}) T_{N,A} + (1 + E_I) - J_{bf} E_I = J_D, \tag{40}$$

$$J_D(1 - \tfrac{5}{2} T_{N,\text{peak}}) = (1 + E_I), \tag{41}$$

and

$$n_{N,\text{peak}} = \tfrac{8}{5}\frac{1}{T_{N,\text{peak}}}. \tag{42}$$

We used the definitions:

$$F \equiv \int_0^L dz \frac{m_e}{m_i}\frac{\nu_d}{v_0}, \quad f \equiv \frac{1}{F}\int_0^{z_{\text{peak}}} dz \frac{m_e}{m_i}\frac{\nu_d}{v_0},$$

$$E_I \equiv \frac{\alpha_i \epsilon_i}{e\phi_A}, \quad T_N \equiv \frac{T}{e\phi_A}, \quad n_N \equiv \frac{n v_0 S m_i}{\dot{m}} \tag{43}$$

and

$$P_A \equiv \frac{(nT)_A S}{\dot{m} v_0}, \quad J_{bf} \equiv \frac{j_{bf} S m_i}{e\dot{m}}. \tag{44}$$

In Eqs. (38)–(42) J_D, J_{bf}, $T_{N,\text{peak}}$, $T_{N,A}$, P_A, $n_{N,\text{peak}}$ and f are functions of F and E_I. The efficiency is

$$\eta_D = \frac{1}{J_D}. \tag{45}$$

The quantity F is not specified by the input parameters only since ν_d may depend on the electron–neutral collisions, which depend on the neutral density. Formally, this would mean that F depends on the unknown J_{bf}.

There are five governing equations for seven unknowns. However, in the two special cases we address here further approximations can be made that reduce the number of unknowns.

A. Zero ion velocity at the anode

In the case of zero ion velocity at the anode the peak of the potential is located at the anode. We, therefore, specify $z_{\text{peak}} = 0$. Also, all ions move towards the cathode, and therefore $j_{bf} = 0$. In the dimensionless equations we write

$$f = 0, \quad T_{N,\text{peak}} = T_{N,A}, \quad P_A = \tfrac{4}{5}, \quad J_{bf} = 0. \tag{46}$$

Examining these relations and Eq. (6) we observe that 4/5 of the thrust $\dot{m} v_0$ are a result of the plasma pressure at the anode and 1/5 only is a result of the magnetic field force. The increase of the efficiency due to the increase of the magnetic field intensity is achieved by reducing the current that generates the magnetic field force.

Equations (38), (41), and (42) become the governing equations for the unknowns J_D, $T_{N,A} = T_{N,\text{peak}}$, and $n_{N,\text{peak}}$. In this case the thin ionization layer is located in the vicinity of the anode and the integration in Eq. (38) spans the entire channel length. Equation (39) is trivially satisfied. Writing the dimensional energy balance equation (36) in the form

$$\frac{\dot{m}}{Sm_i}(e\phi_A+\alpha_i\epsilon_i)+\frac{5}{2}T_A\frac{j_D}{e}=j_D\phi_A, \tag{47}$$

we notice that the electric energy that is dissipated in the thruster is invested in ionizing and accelerating the propellant, and, in addition, part of the electric energy ends up as thermal energy of the electrons that reach the anode. The energy loss in this case is a result of excess electron heating. In fact, by dividing Eq. (47) by $j_D\phi_A$ we can write it as

$$\eta_D=\eta_{D,\max}\left(1-\frac{5}{2}\frac{T_A}{e\phi_A}\right), \tag{48}$$

where

$$\eta_{D,\max}=\frac{1}{1+\alpha_i\epsilon_i/(e\phi_A)}. \tag{49}$$

The maximal efficiency is obtained when $T_A=0$.

Let us express these quantities in terms of F and E_I

$$\frac{T_A}{e\phi_A}=\frac{2}{5}\left(\frac{1-5FE_I}{1+5F}\right), \tag{50}$$

$$n_A=n_{\text{peak}}=4\frac{\dot{m}}{v_0Sm_i}\left(\frac{1+5F}{1-5FE_I}\right), \tag{51}$$

$$J_D=1+\frac{1}{5F}, \tag{52}$$

and

$$\eta_D=1-\frac{1}{1+5F}. \tag{53}$$

The maximal efficiency is obtained when F has its maximal value

$$F=F_{\max}=\frac{1}{5E_I}. \tag{54}$$

Then

$$\frac{T_A}{e\phi_A}=0,\quad n_A\to\infty,\quad J_D=J_{D,\min}=1+E_I,$$

$$\eta_D=\eta_{D,\max}=\frac{1}{1+E_I}. \tag{55}$$

On the other hand, when

$$F\to 0 \tag{56}$$

the various parameters obtain the values

$$\frac{T_A}{e\phi_A}\to\left(\frac{T_A}{e\phi_A}\right)_{\max}=\frac{2}{5},\quad n_A\to 4\frac{\dot{m}}{v_0Sm_i}=2n_s,$$

$$J_D\to\infty,\quad \eta_D\to 0, \tag{57}$$

where n_s is the plasma density at the sonic transition plane, as found above.

B. Backflow towards the anode

In the case of a backflow

$$T_A\ll\alpha_i\epsilon_i,\quad (nT)_A\ll(nT)_{\text{peak}}=\frac{4}{5}\frac{\dot{m}}{S}v_0. \tag{58}$$

Examining these inequalities and Eq. (33) we find that in this case of a backflow the net thrust $\dot{m}v_0$ is imparted by the magnetic field force only. The plasma acquires this thrust in the acceleration region, $(1/5)\dot{m}v_0$ by the magnetic field force and $(4/5)\dot{m}v_0$ by force due to the plasma pressure. However, as seen in Eq. (31), in the backflow region there is a balance between the plasma pressure and the magnetic field force, each one of them equals $(4/5)\dot{m}v_0$, the plasma pressure towards the anode, while the magnetic field force is directed towards the exit. The net contribution to the thrust ends up being due to the magnetic field force only.

Employing Eq. (58) we write Eq. (35) in the form

$$\frac{\dot{m}}{Sm_i}(e\phi_A+\alpha_i\epsilon_i)-\frac{j_{bf}}{e}\alpha_i\epsilon_i=j_D\phi_A. \tag{59}$$

We notice that the electric energy that is dissipated in the thruster is invested in ionizing and accelerating part of the propellant towards the exit, and, in addition, in ionizing the part of the propellant that backflows towards the anode. The energy loss in this case is a result of excess ionization. In fact, we can write the last equation as

$$\eta_D=\eta_{D,\max}\left[1+\frac{J_{bf}\alpha_i\epsilon_i}{e\phi_A+\alpha_i\epsilon_i(1-J_{bf})}\right], \tag{60}$$

$$\eta_{D,\max}=\frac{1}{1+E_I}. \tag{61}$$

The maximal efficiency is obtained when $J_{bf}=0$.

Upon approximating P_A and $T_{N,A}$ by zero in the governing equations [Eqs. (38)–(42)], we are left with five equations for the five unknowns J_D, J_{bf}, $T_{N,\text{peak}}$, $n_{N,\text{peak}}$ and f. Let us express these quantities in terms of F and E_I

$$f=\frac{4E_I}{1+5E_I}, \tag{62}$$

$$J_{bf}=1-\frac{1}{5F}\frac{1+5E_I}{E_I(1+E_I)}, \tag{63}$$

$$T_{N,\text{peak}}=-\frac{2}{5}\frac{J_{bf}}{J_D}E_I=\frac{2}{5}\frac{(1+5E_I)-5FE_I(1+E_I)}{(1+5E_I)+5F(1+E_I)}, \tag{64}$$

$$n_{N,\text{peak}}=-4\frac{J_D}{J_{bf}E_I}=4\frac{\dot{m}}{v_0Sm_i}\frac{5F(1+E_I)+(1+5E_I)}{(1+5E_I)-5FE_I(1+E_I)}, \tag{65}$$

$$J_D=1+\frac{1}{5F}\frac{1+5E_I}{1+E_I}, \tag{66}$$

and

$$\eta_D = 1 - \frac{1+5E_I}{5F(1+E_I)+(1+5E_I)}. \tag{67}$$

The value of f is independent of the value of F; at the limit of intense full ionization, the location of the ionization layer does not depend on the intensity of the magnetic field. This is because, for a specified magnetic field profile, mass flow rate and applied voltage, the magnetic field force exerted on the plasma does not depend on the intensity of the magnetic field. This is discussed further in the next subsection.

The maximal efficiency is obtained when F has its maximal value

$$F = F_{\max} = \frac{1}{5E_I}\frac{1+5E_I}{1+E_I}. \tag{68}$$

Then

$$J_{bf}=0, \quad \frac{T_{\text{peak}}}{e\phi_A}=0, \quad n_{\text{peak}}\to\infty, \quad J_D = J_{D,\min} = 1+E_I,$$

$$\eta_D = \eta_{D,\max} = \frac{1}{1+E_I}. \tag{69}$$

On the other hand, when

$$F \to 0, \tag{70}$$

the various parameters obtain the values

$$J_{bf}\to-\infty, \quad \frac{T_{\text{peak}}}{e\phi_A}\to\left(\frac{T_{\text{peak}}}{e\phi_A}\right)_{\max}=\frac{2}{5},$$

$$n_{\text{peak}}\to 4\frac{\dot{m}}{v_0 S m_i}=2n_s, \quad J_D\to\infty, \quad \eta_D\to 0. \tag{71}$$

In the next subsection we summarize the differences in thrust and efficiency between the two cases.

C. Comparison of thrust and efficiency for the two cases

The limit of intense full ionization with no losses is characterized by a thrust $\dot{m}v_0$ that is determined by the mass flow rate and the applied voltage and is independent of the intensity of the magnetic field. The relative contribution of the magnetic field force to this thrust has fixed values, 1/5 when the ion velocity at the anode is zero (the other 4/5 is due to particle pressure), and a unity when a backflow exists (the thrust is imparted completely by the magnetic field force). Since these fractions are fixed, increasing the magnetic field intensity for fixed values of mass flow rate and applied voltage does not increase the exerted magnetic field force; rather it results in lowering the azimuthal electron current in the plasma that is required for providing the fixed value of magnetic field force for each case. This lower azimuthal current and the associated lower discharge current correspond to a higher efficiency.

Comparing the two cases we find that the minimal discharge current and the maximal efficiency are the same. However, the value of F required to achieve a certain efficiency is lower in the case of zero ion velocity at the anode, which is consistent with the fact that the thrust in this case is only partially due to the magnetic field pressure. Thus, for the same thrust level and efficiency, at a specific applied voltage, the magnetic field intensity (related to the value of F) is expected to be higher when ion backflow is present. This result is exhibited in the contour maps presented shortly.

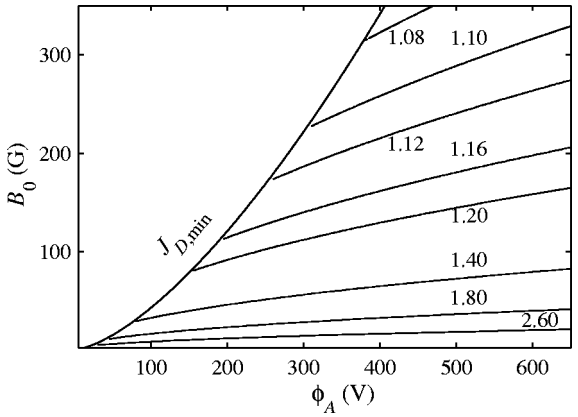

FIG. 3. Contours of equal J_D in the $(\phi_A - B_0)$ plane (zero ion velocity at the anode).

As seen in Eqs. (57) and (71), when the magnetic field intensity is lower and F approaches zero, the discharge current grows asymptotically to infinity. At a constant applied voltage the power needed to accelerate the ions is constant. The excess electrical power applied to the thruster (due to the higher discharge current) is deposited in a finite thermal energy of the electrons that reach the anode ($T = 2/5\ e\phi_A$ for each electron) in the first case, or is used for the generation through ionization of backflow ions ($\alpha_i \epsilon_i$ for each ion) in the second case. Since the number of electrons that reach the anode in the first case and the number of backflow ions in the second case grow with the increasing discharge current, the fraction of power that is not used for thrust generation grows and the efficiency decreases. These results will be demonstrated in the next section as well.

V. APPLICATION OF THE ANALYTICAL RESULTS

In order to show the explicit dependence of the approximated analytical results on the magnetic field intensity and on the applied voltage we need to specify the form of ν_d. In

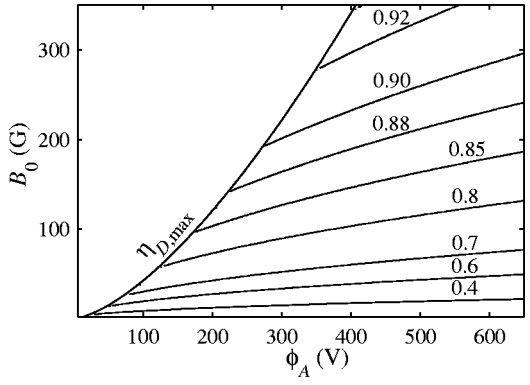

FIG. 4. Contours of equal thruster efficiency η_D in the $(\phi_A - B_0)$ plane (zero ion velocity at the anode).

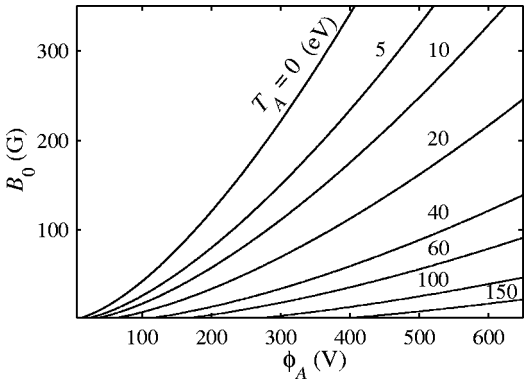

FIG. 5. Contours of equal electron temperature at the anode T_A in the $(\phi_A - B_0)$ plane (zero ion velocity at the anode).

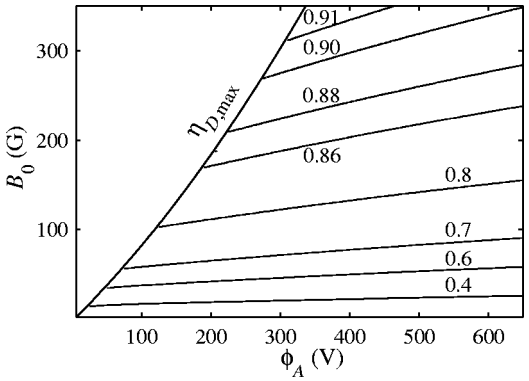

FIG. 7. Contours of equal thruster efficiency η_D in the $(\phi_A - B_0)$ plane (ion backflow case).

large domains of the parameter space $\nu_{ano} \gg \nu_{en}$. Neglecting ν_{en} in the expression for ν_d simplifies the analysis, since then the value of ν_d is determined by the magnetic field intensity only. Although this approximation of neglecting ν_{en} fails when the neutral density is high (for example, when the backflow towards the anode is large), we do make this approximation in the following presentation of the analytical results, so that

$$\nu_d = \frac{\omega_c^2}{\nu_{ano}} = 80\omega_c . \tag{72}$$

Therefore, the value of F is determined by the magnetic field profile $B(z)$ and by ϕ_A.

For the magnetic field profile [Eq. (16)] and for the same values of z_m, L_m, and L as in Sec. II, F takes the form

$$F = 40\sqrt{\pi} B_0 L_m \left(\frac{e}{2\phi_A m_i}\right)^{1/2} \left[\operatorname{erf}\left(\frac{L - z_m}{L_m}\right) - \operatorname{erf}\left(\frac{-z_m}{L_m}\right)\right]$$
$$= 1550 B_0 \phi_A^{-1/2}, \tag{73}$$

where erf denotes the error function. Also, for the values of α_i and ϵ_i as taken above for xenon, E_I becomes

$$E_I = \frac{30}{\phi_A}. \tag{74}$$

In the last two equations B_0 and ϕ_A are expressed in Tesla and in Volts. By specifying the values of B_0 and ϕ_A we determine the values of F and of E_I. For the case of zero ion velocity at the anode we calculate, using Eqs. (50), (52), and (53), the values of J_D, η_D, and $T_A/e\phi_A$. Figures 3–5 show the contour lines of these quantities in the $(\phi_A - B_0)$ plane. The line of $T_A = 0$ bounds the region in the plane in which solutions exist. For the case of a backflow we calculate, using Eqs. (62), (63), (66), and (67), the values of f, J_{bf}, J_D, and η_D. Once f is found, we can calculate the location of the ionization layer z_{peak} via

$$f = 0.553\left[\operatorname{erf}\left(\frac{z_{\text{peak}}}{20} - 1\right) + 0.843\right]. \tag{75}$$

The quantity f (and therefore, also z_{peak}) is a function of the applied voltage ϕ_A only and is independent of B_0. Figures 6–8 show the contour lines of J_D, η_D, and J_{bf} in the $(\phi_A - B_0)$ plane. Figure 9 shows z_{peak} as a function of ϕ_A. As can be seen in the figure, the location of the ionization layer moves towards the anode as the applied voltage increases. The line $J_{bf} = 0$ bounds the regions in the plane in which solutions exist.

As can be seen in Figs. 3 and 6 the discharge current J_D decreases as B_0 is increased or as ϕ_A is decreased. Formally, this decrease expresses the decrease of J_D with the increase of F. Physically, this is because a high B_0 and low azimuthal current (that result in a low J_D) provide the same magnetic field force and thrust as do a low B_0 and high azimuthal current (that results in a high J_D). When ϕ_A is decreased for

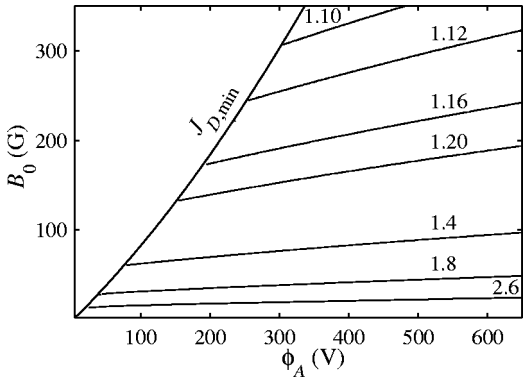

FIG. 6. Contours of equal J_D in the $(\phi_A - B_0)$ plane (ion backflow case).

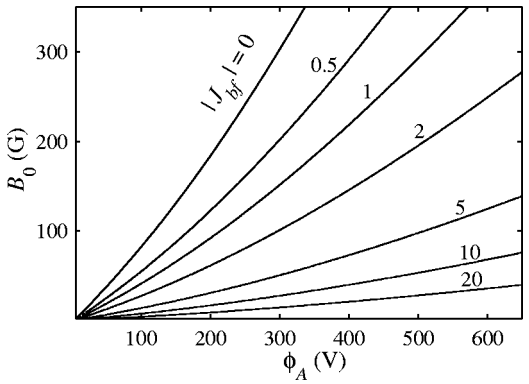

FIG. 8. Contours of equal ion backflow current density $|J_{bf}|$ in the $(\phi_A - B_0)$ plane (ion backflow case).

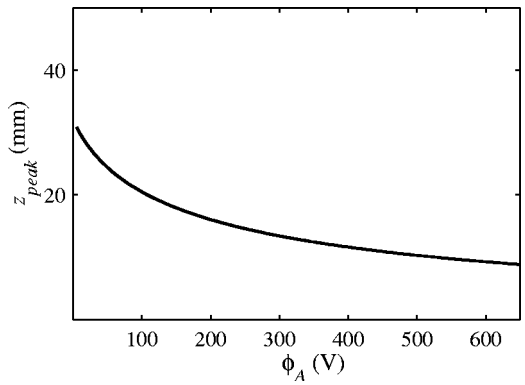

FIG. 9. The location of the peak of the potential z_{peak} as a function of the applied voltage ϕ_A.

a fixed mass flow rate the thrust is decreased (because v_0 is decreased), and therefore for the same B_0 a lower azimuthal current (that results in a lower J_D) is needed in order to provide the smaller required magnetic field force.

Although the neglect of wall losses in our model prevents a quantitative agreement between the model predictions and the experimental results, the general Hall thruster behavior predicted by the analytical model corresponds well to the behavior of experimental thrusters. The analytical model predicts that the discharge current decreases with increasing magnetic field intensity until a maximal magnetic field intensity is reached, beyond which no steady state solution exists. In a typical Hall thruster experiment the discharge current is measured as a function of the magnetic field intensity for a constant applied voltage. In most cases, such as in the Soreq laboratory model Hall thruster,[2,22] the discharge current does indeed decrease as the magnetic field intensity is increased until a minimal discharge current is obtained. Further increase of the magnetic field intensity results in severe discharge current oscillations which drastically reduce the thruster efficiency and pose an upper limit on the magnetic field intensity at which a steady state operation is still possible. Furthermore, as the analytical model predicts, the maximal magnetic field intensity, i.e., the intensity yielding the minimal discharge current, increases as the applied voltage is increased.

A comparison of the analytical and the numerical results is presented in Fig. 10. Shown are J_D, η_C, T_{peak}, and J_{bf} as a function of the magnetic field intensity B_0, for a fixed value of the applied voltage ($\phi_A = 300$ V). The comparison is made for the two cases: Zero ion velocity at the anode and an ion backflow. The numerical results exhibit the same trends as do the analytical results. The analytical model predicts a somewhat higher efficiency than the numerical calculation does. The small discrepancy is a result of the neglect in the analytical model of the finite thickness of the ionization layer and of the finite electron and ion energies at the anode in the backflow case. The analytical model also predicts a lower value of B_0 for achieving a certain efficiency and, consequently, a lower maximal possible value of B_0. This is also a result of the neglect of certain losses in the analytical model. Generally, the comparison between the

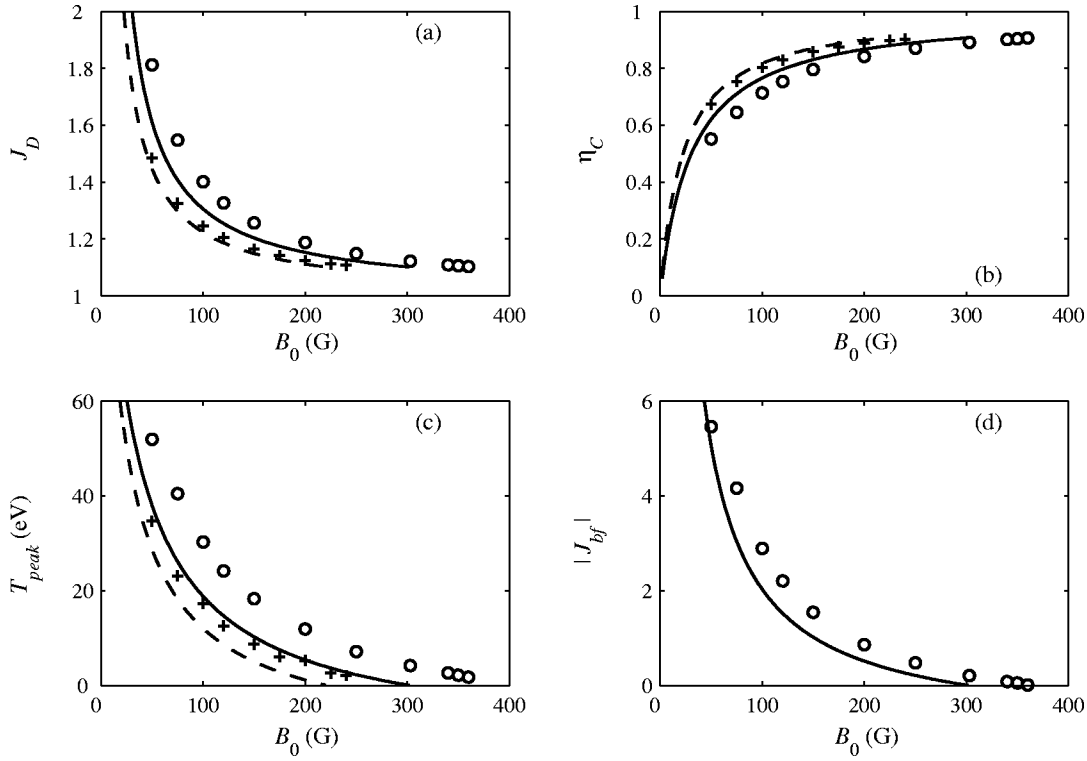

FIG. 10. A comparison of analytical and numerical results for both zero ion velocity and ion backflow at the anode. The values of the parameters are: $S = 45$ cm^2, $L = 50$ mm, $z_m = 20$ mm, $L_m = 20$ mm, $\dot{m} = 5.32$ mg/s, $\phi_A = 300$ V, $\alpha_i = 2.5$. Zero ion velocity at the anode: Analytical prediction—dashed, numerical calculation—plus signs. Ion backflow: Analytical prediction—solid, numerical calculation—circles. The quantity T_{peak} is the temperature at the peak of the potential and not the peak of the temperature.

analytical and the numerical results exhibits a fairly good agreement, demonstrating the usefulness of the analytical model in guiding more elaborate models.

VI. CONCLUSIONS

The flow in the Hall thruster was analyzed at the limit of intense full ionization, for the ideal case of negligible wall losses and heat conductivity. Two kinds of flows were examined; a flow in which the ion velocity at the anode is zero and a flow with an ion backflow towards the anode. We were able to derive analytic expressions for certain important flow parameters as a function of the control parameters, while we leave open the question of what the boundary condition at the anode should be. The analytical expressions agree well with numerical solutions of the equations and predict operational features similar to the actual device.

The dependence of the efficiency on the input parameters, such as the applied voltage and the magnetic field intensity, was found to be similar in both flows. The main difference between the two kinds of flow is the mechanism of energy losses. In the case of a zero ion velocity at the anode, energy is lost through the finite temperature with which electrons reach the anode. In the case of an ion backflow, energy is lost in the ionization of the backflow ions, which undergo recombination at the anode. A flow with a zero ion velocity at the anode (no ion backflow) may be advantageous since a lower magnetic field intensity is required in order to achieve a certain efficiency. On the other hand, the acceleration region in this regime is longer and wall losses may reduce the performance.

The analytical results presented here help to better understand the thruster behavior and the dependence of the efficiency on the input parameters. The analytical model should be useful in guiding more elaborate models that take into account additional important processes, such as heat conductivity and ion losses in lateral walls. These processes are known to extend the thickness of the ionization layer, to moderate the intensity of the ionization and to reduce the electron temperature and the efficiency to more realistic values.

ACKNOWLEDGMENTS

The authors are grateful to Professor N. J. Fisch and to G. Makrinich for helpful discussions.

This research has been partially supported by a Grant No. 1370 from the Israel Ministry of Science Culture and Sport (through the Israel Space Agency) and by a Grant No. 9800145 from the United States-Israel Binational Science Foundation (BSF), Jerusalem, Israel.

[1] A. I. Morozov, Yu. V. Esipchuk, G. N. Tilinin, A. V. Trofinov, Yu. A. Sharov, and G. Ya. Shahepkin, Sov. Phys. Tech. Phys. **17**, 38 (1972).
[2] J. Ashkenazy, Y. Raitses, and G. Appelbaum, Phys. Plasmas **5**, 2055 (1998).
[3] V. V. Zhurin, H. R. Kaufman, and R. S. Robinson, Plasma Sources Sci. Technol. **8**, R1 (1999).
[4] A. Fruchtman, N. J. Fisch, J. Ashkenazy, and Y. Raitses, IEPC Paper No. 97-022, *25th International Electric Propulsion Conference*, Cleveland, OH (Electric Rocket Propulsion Society, Cleveland, OH, 1997).
[5] A. Fruchtman and N. J. Fisch, AIAA Paper No. 98-3500, *34th Joint Propulsion Conference*, Cleveland, OH (American Institute of Aeronautics and Astronautics, Washington, DC, 1998).
[6] A. Cohen-Zur, A. Fruchtman, and J. Ashkenazy, IEPC Paper No. 99-108, *26th International Electric Propulsion Conference*, Kitakyushu, Japan (Japan Society of Aeronautical and Space Sciences, 1999).
[7] A. Fruchtman, N. J. Fisch, and Y. Raitses, Phys. Plasmas **8**, 1048 (2001).
[8] E. Ahedo and M. Martinez-Sanchez, AIAA Paper No. 98-8788, *34th Joint Propulsion Conference*, Cleveland, OH (American Institute of Aeronautics and Astronautics, Washington, DC, 1998).
[9] K. Makowski, Z. Peradzynski, N. Gascon, and M. Dudeck, AIAA Paper No. 99-2295, *35th Joint Propulsion Conference*, Los Angeles, CA (American Institute of Aeronautics and Astronautics, Washington, DC, 1999).
[10] V. Yu. Fedotov, A. A. Ivanov, G. Guerrini, A. N. Vesselovzorov, and M. Bacal, Phys. Plasmas **6**, 4360 (1999).
[11] E. Ahedo, P. Martinez-Cerezo, and M. Martinez-Sanchez, Phys. Plasmas **8**, 3058 (2001).
[12] J. Sankovic, J. Hamley, and T. Hang, IEPC Paper No. 93-094, *23rd International Electric Propulsion Conference*, Seattle, WA (Electric Rocket Propulsion Society, Cleveland, OH, 1993).
[13] E. Ahedo, P. Martinez-Cerezo, J. M. Gallardo, and M. Martinez-Sanchez, IEPC Paper No. 01-017, *27th International Electric Propulsion Conference*, Pasadena, CA (Electric Rocket Propulsion Society, Cleveland, OH, 2001).
[14] E. Y. Choueiri, Phys. Plasmas **8**, 5025 (2001).
[15] M. Keidar, I. D. Boyd, and I. I. Beilis, Phys. Plasmas **8**, 5315 (2001).
[16] A. I. Morozov and L. S. Solov'ev, *Steady-state Plasma Flow in a Magnetic Field*, in *Reviews of Plasma Physics*, edited by M. A. Leontovich (Consultants Bureau, New York, 1980), Vol. 8, p. 1.
[17] D. Bohm, in *The characteristics of Electrical Discharges in Magnetic Fields*, edited by A. Guthry and R. K. Wakerling (McGraw-Hill, New York, 1949), Chap. 3.
[18] A. Bishaev and V. Kim, Sov. Phys. Tech. Phys. **23**, 1055 (1978).
[19] V. Kim, J. Propul. Power **14**, 736 (1998).
[20] L. Dorf, V. Semenov, Y. Raitses, and N. J. Fisch, AIAA Paper No. 2002-4246, *38th Joint Propulsion Conference*, Indianapolis, IN (American Institute of Aeronautics and Astronautics, Washington, DC, 2002).
[21] M. A. Lieberman and A. J. Lichtenberg, *Principles of Plasma Discharges and Materials Processing* (Wiley, New York, 1994).
[22] Y. Raitses, *Investigations of the Hall Thruster and Its Use for Satellite Drag Compensation*, D.Sc. thesis (Technion-Israel Institute of Technology, Israel, 1997).